

# A simplified view of blazars: the neutrino background

P. Padovani<sup>1,2\*</sup>, M. Petropoulou<sup>3†</sup>, P. Giommi<sup>4,5</sup>, E. Resconi<sup>6</sup>

<sup>1</sup>European Southern Observatory, Karl-Schwarzschild-Str. 2, D-85748 Garching bei München, Germany

<sup>2</sup>Associated to INAF - Osservatorio Astronomico di Roma, via Frascati 33, I-00040 Monteporzio Catone, Italy

<sup>3</sup>Department of Physics and Astronomy, Purdue University, 525 Northwestern Avenue, West Lafayette, IN 47907, USA

<sup>4</sup>ASI Science Data Center, via del Politecnico s.n.c., I-00133 Roma Italy

<sup>5</sup>ICRANet-Rio, CBPF, Rua Dr. Xavier Sigaud 150, 22290-180 Rio de Janeiro, Brazil

<sup>6</sup>Technische Universität München, Physik-Department, James-Frank-Str. 1, D-85748 Garching bei München, Germany

Accepted ... Received ...; in original form ...

## ABSTRACT

Blazars have been suggested as possible neutrino sources long before the recent IceCube discovery of high-energy neutrinos. We re-examine this possibility within a new framework built upon the *blazar simplified view* and a self-consistent modelling of neutrino emission from individual sources. The former is a recently proposed paradigm that explains the diverse statistical properties of blazars adopting minimal assumptions on blazars' physical and geometrical properties. This view, tested through detailed Monte Carlo simulations, reproduces the main features of radio, X-ray, and  $\gamma$ -ray blazar surveys and also the extragalactic  $\gamma$ -ray background at energies  $\gtrsim 10$  GeV. Here we add a hadronic component for neutrino production and estimate the neutrino emission from BL Lacs as a class, “calibrated” by fitting the spectral energy distributions of a pre-selected sample of BL Lac objects and their (putative) neutrino spectra. Unlike all previous papers on this topic, the neutrino background is then derived by summing up at a given energy the fluxes of each BL Lac in the simulation, all characterised by their own redshift, synchrotron peak energy,  $\gamma$ -ray flux, etc. Our main result is that BL Lacs as a class can explain the neutrino background seen by IceCube above  $\sim 0.5$  PeV while they only contribute  $\sim 10\%$  at lower energies, leaving room to some other population(s)/physical mechanism. However, one cannot also exclude the possibility that individual BL Lacs still make a contribution at the  $\approx 20\%$  level to the IceCube low-energy events. Our scenario makes specific predictions testable in the next few years.

**Key words:** neutrinos — radiation mechanisms: non-thermal — BL Lacertae objects: general — gamma-rays: galaxies

## 1 INTRODUCTION

Blazars are a class of Active Galactic Nuclei (AGN), which host a jet oriented at a small angle with respect to the line of sight. Highly relativistic particles moving within the jet and in a magnetic field emit non-thermal radiation (Blandford & Rees 1978; Urry & Padovani 1995). This is at variance with most other AGN whose energy is mainly thermal and produced through accretion of matter onto a supermassive black hole. Because of their peculiar orientation and highly relativistic state, blazars are characterised by distinctive and extreme observational properties, including superluminal motion, large

and rapid variability, and strong emission over the entire electromagnetic spectrum. The two main blazar subclasses, namely BL Lacertae objects (BL Lacs) and flat-spectrum radio quasars (FSRQ), differ mostly in their optical spectra, with the latter displaying strong, broad emission lines and the former instead being characterised by optical spectra showing at most weak emission lines, sometimes exhibiting absorption features, and in many cases being completely featureless.

The spectral energy distributions (SEDs) of blazars are composed of two broad humps, a low-energy and a high-energy one. The peak of the low-energy hump ( $\nu_{\text{peak}}^S$ ) can occur at widely different frequencies, ranging from about  $\sim 10^{12.5}$  Hz ( $\sim 0.01$  eV) to  $\sim 10^{18.5}$  Hz ( $\sim 13$  keV). The high-energy hump, which may extend up to  $\sim 10$  TeV, has a peak energy that ranges between  $\sim 10^{20}$  Hz

\* E-mail: ppadovan@eso.org

† Einstein Postdoctoral Fellow

( $\sim 0.4$  MeV) to  $\sim 10^{26}$  Hz ( $\sim 0.4$  TeV) (Giommi et al. 2012b; Arsioli et al. 2015). Based on the rest-frame value of  $\nu_{\text{peak}}^S$ , BL Lacs can be further divided into Low energy peaked (LBL) sources ( $\nu_{\text{peak}}^S < 10^{14}$  Hz [ $< 0.4$  eV]), Intermediate ( $10^{14}$  Hz  $< \nu_{\text{peak}}^S < 10^{15}$  Hz [ $0.4$  eV  $< \nu_{\text{peak}}^S < 4$  eV]) and High ( $\nu_{\text{peak}}^S > 10^{15}$  Hz [ $> 4$  eV]) energy peaked (IBL and HBL) sources respectively (Padovani & Giommi 1995). It is generally accepted that the low-energy blazar emission is the result of electron synchrotron radiation, with the peak frequency reflecting the maximum energy at which electrons can be accelerated (e.g. Giommi et al. 2012b). On the other hand, the origin of their high-energy emission is still under debate. In the conventional leptonic scenarios,  $\gamma$ -ray emission is thought to be due to inverse Compton radiation (e.g. Maraschi et al. 1992; Sikora et al. 1994) whereas in leptohadronic scenarios it may be the result of proton synchrotron radiation (Aharonian 2000; Mücke & Protheroe 2001) or may have a photohadronic origin (e.g. Petropoulou et al. 2015, and references therein). Given that the presence of relativistic electrons is necessary to explain at least the low-energy hump of the SED, it is reasonable to assume that proton acceleration takes also place in blazar jets (Biermann & Strittmatter 1987; Sironi et al. 2013; Globus et al. 2014 and references, therein). Although leptohadronic models bear several attractive features from the theoretical point of view (e.g. Halzen & Zas 1997), these are not sufficient to rule out leptonic models. The most promising way to settle the issue of proton acceleration in blazars is through high-energy neutrino experiments, since neutrino emission is an unavoidable outcome of leptohadronic models.

Padovani & Resconi (2014) have recently extended the domain over which blazars could be relevant astrophysical sources into neutrino territory. Namely, on the basis of a joint positional and energetic diagnostic, they have suggested a possible association between eight BL Lacs (all HBL) and seven neutrino events reported by the IceCube collaboration (IceCube Collaboration 2014). Following up on this idea, Petropoulou et al. (2015) have modelled the SEDs of six of these BL Lacs using a one-zone leptohadronic model and mostly nearly simultaneous data. The neutrino flux for each BL Lac was self-consistently calculated, using photon and proton distributions specifically derived for every individual source. The SEDs of the sources, although different in shape and flux, were all well fitted by the model using reasonable parameter values. Moreover, the model-predicted neutrino flux and energy for these sources were of the same order of magnitude as those of the IceCube neutrinos. In two cases, i.e. MKN 421 and H 1914–194, a suggestively good agreement between the model prediction and the neutrino flux was found.

The hypothesis put forward by Padovani & Resconi (2014) and Petropoulou et al. (2015), if correct, should materialise in an IceCube detection but this has not happened yet. At present, in fact, IceCube has not identified any point sources and therefore its signal remains unresolved, although the published upper limits are still not ruling out the scenario described above (Padovani & Resconi 2014).

In this paper we aim to calculate the cumulative neu-

trino emission from *all* BL Lacs within the leptohadronic scenario for their  $\gamma$ -ray emission in order to see if BL Lacs *as a class* can indeed explain the IceCube detections. By considering only the neutrino emission produced in the blazar jet, we calculate the neutrino background<sup>1</sup> (NBG) from blazars. This is the most conservative estimate, since we do not take into account the ‘cosmogenic’ neutrino production due to the propagation of escaping cosmic rays (CRs) in the intergalactic medium (Ahlers & Halzen 2012). As discussed below, calculating the NBG from blazars requires a very detailed knowledge of the blazar population in terms of  $\nu_{\text{peak}}^S$ ,  $\gamma$ -ray fluxes, redshift, etc. All these parameters, and many more, are available in the simulations done in a series of papers by Giommi, Padovani, and collaborators.

Giommi et al. (2012a) (hereafter Paper I) have proposed a new blazar paradigm where blazars are classified into FSRQ and BL Lacs according to a varying mix of the Doppler-boosted radiation from the jet, the emission from the accretion disc, the broad-line region, and the light from the host galaxy. This is also based on minimal assumptions on the physical properties of the non-thermal jet emission, and unified schemes. These posit that BL Lacs and FSRQ are simply low-excitation (LERGs)/Fanaroff-Riley (FR) I and high-excitation (HERGs)/FR II radio galaxies with their jets forming a small angle with respect to the line of sight (e.g. Urry & Padovani 1995). They called this new approach the *blazar simplified view* (BSV). By means of detailed Monte Carlo simulations, Paper I showed that the BSV scenario is consistent with the complex observational properties of blazars as we know them from all the surveys carried out so far in the radio and X-ray bands, solving at the same time a number of long-standing issues.

In a subsequent paper (Giommi, Padovani, & Polenta 2013, hereafter Paper II) the Monte Carlo simulations were extended to the  $\gamma$ -ray band (100 MeV – 100 GeV) and found to match very well the observational properties of blazars in the *Fermi*-LAT 2-yr source catalogue (Nolan et al. 2012; Ackermann et al. 2011) and the *Fermi*-LAT data of a sample of radio selected blazars (Giommi et al. 2012b; Planck Collaboration 2011).

Padovani & Giommi (2015) (hereafter Paper III) considered the case of very high energy (VHE) emission ( $E > 100$  GeV) extrapolating from the expectations for the GeV band, and made detailed predictions for current and future Cherenkov facilities, including the Cherenkov Telescope Array. Finally, Giommi & Padovani (2015) (hereafter Paper IV) have extended the predictions below the sensitivity of current surveys and estimated the contribution of blazars to the X-ray and  $\gamma$ -ray extragalactic backgrounds. They found that the integrated light from blazars can explain the cosmic background at energies  $\gtrsim$

<sup>1</sup> We use “background” in the astronomical sense of total emission from a population of astrophysical objects. This includes resolved and unresolved sources, the contribution of the latter corresponding to the “diffuse” intensity generally referred to by high-energy physicists.

10 GeV, and contribute  $\approx 40 - 70\%$  of the  $\gamma$ -ray diffuse radiation in the 0.1 – 10 GeV band.

The purpose of this paper is to merge the simulation and theoretical approaches by adding to the former a hadronic “prior” necessary for the neutrino emission, as detailed in Sect. 3. As in papers I – IV we use a  $\Lambda$ CDM cosmology with  $H_0 = 70 \text{ km s}^{-1} \text{ Mpc}^{-1}$ ,  $\Omega_m = 0.27$  and  $\Omega_\Lambda = 0.73$  (Komatsu et al. 2011).

## 2 THEORETICAL MODELLING

Neutrino production is studied within a specific theoretical framework for blazar emission where photohadronic interactions have an active role in shaping the blazar SED, as detailed in Petropoulou et al. (2015). In their model, the low-energy emission of the blazar SED is attributed to synchrotron radiation of relativistic electrons, whereas the observed high-energy (GeV – TeV) emission has a photohadronic origin. Under the assumption that proton acceleration to high energies ( $\sim 10^{16} - 10^{17} \text{ eV}$ ) is also viable in blazar jets, the production of charged pions is a natural outcome of photopion ( $p\pi$ ) interactions between the relativistic protons and the internally produced synchrotron photons. The decay of charged pions results in the injection of secondary relativistic electron-positron pairs<sup>2</sup>. It is the synchrotron radiation of the latter that emerges in the GeV – TeV regime, in contrast to the hadronic cascade scenario for blazar emission (Mannheim et al. 1991; Mannheim 1993), where the cascade emission mainly contributes to the  $\gamma$ -ray regime<sup>3</sup>. As the synchrotron self-Compton emission from primary electrons may also emerge in the GeV – TeV energy band, the observed  $\gamma$ -ray emission can be totally or partially explained by photohadronic processes, depending on the specifics of individual sources (Petropoulou et al. 2015). Since the luminosity of the  $p\pi$  component is directly connected to that of very high-energy ( $\sim 2 - 20 \text{ PeV}$ ) neutrinos, our approach allows us to associate the observed  $\gamma$ -ray blazar flux with the expected neutrino flux. The physical model we use has been described, in more general terms, by Dimitrakoudis et al. (2012) and Dimitrakoudis, Petropoulou, & Mastichiadis (2014).

## 3 MONTE CARLO SIMULATIONS

In the first two papers of this series we presented the principles on which the BSV is built and mostly concentrated on the statistical properties of blazars, such as distribution trends, average values of some important parameters, and compared those with observed distributions and values in radio and X-ray surveys. In Paper III we tied our simulation to the absolute numbers of the *Fermi*-2LAC catalogue and predicted the number of

sources in the VHE band taking into account the extragalactic background light (EBL) absorption. In Paper IV we calculated the integrated flux from the entire population of blazars of different types in the X-ray and  $\gamma$ -ray bands.

For the reader’s convenience we briefly summarise here our Monte Carlo simulations covering the radio through the  $\gamma$ -ray bands, which are based on a number of ingredients, including: the (radio) blazar luminosity function and evolution, a distribution of the Lorentz factor of the electrons and of the Doppler factor, a synchrotron model, an accretion disk component, the host galaxy, plus a series of  $\gamma$ -ray constraints based on observed distributions estimated using simultaneous multi-frequency data: the distribution of the ratio between high-energy and low-energy hump fluxes, the dependence of the  $\gamma$ -ray spectral index on  $\nu_{\text{peak}}^S$ , and that of the  $\gamma$ -ray flux on radio flux density. Sources are classified as BL Lacs, FSRQ, or radio galaxies based on the optical spectrum, as in real surveys. Readers are referred to Paper I and II for full details. We stress that no assumption has been made in the simulations about the process responsible for the  $\gamma$ -ray emission.

As done in Paper III the SEDs were extrapolated to the VHE band by using our simulated *Fermi* fluxes and spectral indices and assuming a break at  $E = E_{\text{break}}$  and a steepening of the photon spectrum by  $\Delta\Gamma$ . Our adopted values were  $E_{\text{break}} = 100 \text{ GeV}$  and  $\Delta\Gamma = 1$  and  $E_{\text{break}} = 200 \text{ GeV}$  and  $\Delta\Gamma = 0.5$ , the latter being our default choice. VHE spectra were attenuated using recent estimates of the EBL absorption as a function of redshift (Domínguez et al. 2011).

### 3.1 The neutrino component

The Monte Carlo simulations described above characterise fully the *photon* emission from the BL Lac population. To get to the neutrinos, we need to add a hadronic “prior”, which is built on the knowledge gained by fitting the SEDs of six individual BL Lac sources and their respective neutrino spectra in Petropoulou et al. (2015).

We model the observed differential neutrino plus anti-neutrino ( $\nu + \bar{\nu}$ ) energy flux of all flavours ( $F_\nu(E_\nu)$ ) as

$$F_\nu(E_\nu) = F_0 E_\nu^{-s} \exp\left(-\frac{E_\nu}{E_0}\right), \quad (1)$$

where the parameters to be defined are  $E_0$  (characteristic energy),  $s$  (spectral slope), and  $F_0$  (normalisation).

#### 3.1.1 Determination of $E_0$

We set the characteristic energy  $E_0$  equal to the peak energy of the neutrino spectrum  $E_{\nu,p}$ , which, in good approximation, can be written as

<sup>2</sup> We will commonly refer to them as electrons.

<sup>3</sup> The cascade is initiated by photon-photon absorption of very high-energy  $\gamma$ -rays ( $\gg \text{TeV}$ ), which, in turn, are produced by synchrotron radiation of secondary pairs from pion decays and Bethe-Heitler ( $p\pi$ ) pair production.

$$E_{\nu,p}(\delta, z, \nu_{\text{peak}}^S) \simeq \frac{17.5 \text{ PeV}}{(1+z)^2} \left( \frac{\delta}{10} \right)^2 \left( \frac{\nu_{\text{peak}}^S}{10^{16} \text{ Hz}} \right)^{-1}, \quad (2)$$

$$E_0 = E_{\nu,p}$$

where  $\delta$  is the Doppler factor and  $z$  is the source redshift (e.g. Dermer, Ramirez-Ruiz, & Le 2007). Here  $\nu_{\text{peak}}^S$  is the *observed* synchrotron peak frequency. This relation is valid as long as protons energetic enough to produce pions by interacting with the photons of the low-energy (synchrotron) hump of the SED can be accelerated in the jet. We assume that this condition is satisfied in all BL Lacs and discuss possible caveats in Sect. 5.2.

Equation 2 requires as input  $z$ ,  $\delta$ , and  $\nu_{\text{peak}}^S$ . These are all part of the output of the simulations so  $E_0$  can be easily derived source by source.

### 3.1.2 Determination of $s$

In Petropoulou et al. (2015) the neutrino spectra from six BL Lac objects were calculated self-consistently. It was shown that all neutrino spectra peaked at  $\sim E_{\nu,p}$  and  $E_\nu F_\nu(E_\nu) \propto E_\nu^{-s+1}$  with  $\langle s \rangle \simeq -0.35$ , namely the neutrino spectra are relatively flat. This is not a matter of fine tuning or coincidence as, in our scenario, the number density of the target photons decreases with photon energy<sup>4</sup>. Based on the range of values found by Petropoulou et al. (2015), the neutrino slope  $s$  was drawn from a Gaussian distribution centred at  $-0.35$  with  $\sigma = 0.12$ .

### 3.1.3 Determination of $F_0$

The normalisation  $F_0$  is given by

$$F_0 = \frac{F_{\nu,\text{tot}} E_{\nu,p}^{s-1}}{\int_{x_{\min}}^{\infty} dx x^{-s} e^{-x}}, \quad (3)$$

where  $x \equiv E_\nu/E_{\nu,p}$  and  $x_{\min}$  is the minimum normalised neutrino energy. Because of the neutrino spectral shape, it is safe to set  $x_{\min} = 0$ , and the integral reduces to the  $\Gamma$  function with argument  $1-s$ . In our approach, the integrated neutrino flux is associated to the integrated  $\gamma$ -ray flux as

$$F_{\nu,\text{tot}} = Y_{\nu\gamma} F_\gamma(> E_\gamma), \quad (4)$$

where we chose  $E_\gamma = 10 \text{ GeV}$ <sup>5</sup>. By construction,  $Y_{\nu\gamma}$  encloses all the information on the optical depth for photopion interactions and the proton luminosity.

<sup>4</sup> This can be understood as follows: we assume that the proton distribution extends up to  $\gamma_{p,\text{max}} \gtrsim \gamma_{p,\text{th}}$ , where  $\gamma_{p,\text{th}}$  is the threshold energy for  $p\pi$  interactions with synchrotron photons of frequency  $\nu_{\text{peak}}^S$ . Protons with  $\gamma_p < \gamma_{p,\text{th}}$ , which pion-produce on synchrotron photons with  $\nu > \nu_{\text{peak}}^S$ , are responsible for the production of neutrinos with energies  $E_\nu < E_{\nu,p}$ . Thus, the neutrino spectrum below its peak energy probes the soft part of the low-energy hump of the SED.

<sup>5</sup> Our results are totally independent of this choice.

It has an upper limit, i.e.  $Y_{\nu\gamma} \sim 3$ , which is obtained when synchrotron emission from  $p\pi$  pairs accounts for the whole observed  $\gamma$ -ray flux (e.g. Petropoulou & Mastichiadis 2015). To reach this result, we also made some simple assumptions about the pion production ratio and the energy of the leptons produced from the pion decay chain. However, there is no lower limit on  $Y_{\nu\gamma}$ :  $Y_{\nu\gamma} \ll 1$  simply implies a leptonic origin for the  $\gamma$ -ray blazar emission. Application of the lepto-hadronic model to individual BL Lacs with different properties, such as SED and redshift, resulted in  $Y_{\nu\gamma}$  values covering the range  $0.1 - 2$  (Petropoulou et al. 2015).

Based on the results of Petropoulou et al. (2015), and assuming that  $Y_{\nu\gamma}$  is the same independently of BL Lac class (but see Sect. 5.2.1) we adopt two different options for the ratio  $Y_{\nu\gamma}$ :

(i) we assume a constant value for all BL Lacs,  $Y_{\nu\gamma} = 0.8$ , which is the average derived from the modelling of the six BL Lacs;

(ii) we use a relation between  $Y_{\nu\gamma}$  and the observed  $\gamma$ -ray luminosity above 10 GeV in  $\text{erg s}^{-1}$ ,  $L_\gamma(> 10 \text{ GeV})$ , i.e.  $\log Y_{\nu\gamma} = -0.58 \times \log L_\gamma(> 10 \text{ GeV}) + 26.3$ , with  $Y_{\nu\gamma} \leq 3$ . This is a simple fit to the values in Petropoulou et al. (2015) (see their Fig. 11) motivated by the possible trend found in the sample of six BL Lacs. In practice, this translates to  $Y_{\nu\gamma} = 3$  for  $L_\gamma(> 10 \text{ GeV}) < 3 \times 10^{44} \text{ erg s}^{-1}$ , that is for basically all LBL and  $\sim 80\%$  of HBL.

Combining all of the above, we derive the final expression for the observed neutrino flux expected from each BL Lac object ( $E^2 dN/dE$  units):

$$E_\nu F_\nu(E_\nu) = \frac{Y_{\nu\gamma} F_\gamma(> 10 \text{ GeV})}{\int_{x_{\min}}^{\infty} dx x^{-s} e^{-x}} \left( \frac{E_\nu}{E_{\nu,p}} \right)^{-s+1} \exp\left(-\frac{E_\nu}{E_{\nu,p}}\right). \quad (5)$$

The neutrino fluxes at various energies were then calculated based on this spectrum, which in turn depends on  $E_{\nu,p}$ ,  $s$ , and  $Y_{\nu\gamma}$ , and the  $\gamma$ -ray flux and power from the simulations. Since  $E_{\nu,p}$  is fully determined by eq. 2 and  $s$  covers a narrow range, we are left only with  $Y_{\nu\gamma}$  as a possible “tuneable” parameter (see Sect. 5.5).

Finally, the total NBG was computed as  $B = \int_{F_{\min}}^{F_{\max}} F \frac{dN}{dF} dF$  where  $\frac{dN}{dF}$  are the differential number counts and  $F_{\min}$  and  $F_{\max}$  are the fluxes over which these extend. Since the IceCube data are “per neutrino flavour” our numbers, which refer to all neutrino flavours, were divided by three<sup>6</sup>. Ten simulations were run and the average was then calculated to smooth out the “noise” inherent to the Monte Carlo process.

<sup>6</sup> The neutrino flux produced at the source contains neutrinos of different flavours with an approximate ratio  $F_{\nu_e} : F_{\nu_\mu} : F_{\nu_\tau} = 2 : 1 : 0$ . However, by the time they reach Earth their ratio will have changed to  $F_{\nu_e} : F_{\nu_\mu} : F_{\nu_\tau} = 1 : 1 : 1$  due to neutrino oscillations (Learned & Pakvasa 1995), as indeed observed (Aartsen et al. 2015).

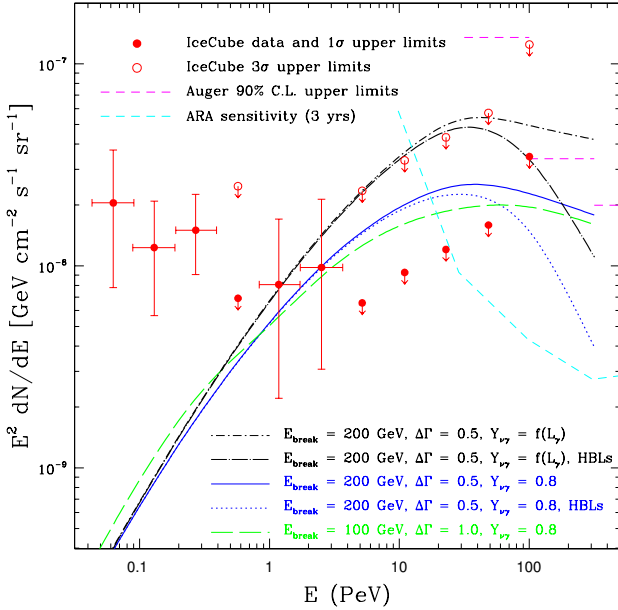


**Figure 1.** The predicted neutrino ( $\nu + \bar{\nu}$ ) background per neutrino flavour from BL Lacs. Different lines correspond to different assumptions (starting from the top):  $Y_{\nu\gamma}$  anti-correlated with  $L_\gamma (> 10 \text{ GeV})$  for all BL Lacs (black dot short-dashed line) and HBL (black dot long-dashed line);  $Y_{\nu\gamma} = 0.8$  and  $E_{\text{break}} = 200 \text{ GeV}$ ,  $\Delta\Gamma = 0.5$ , for all BL Lacs (blue solid line) and HBL (blue dotted line);  $Y_{\nu\gamma} = 0.8$  and  $E_{\text{break}} = 100 \text{ GeV}$ ,  $\Delta\Gamma = 1$ , for all BL Lacs (green long dashed line). All lines correspond to the mean value of ten different simulations. The (red) filled points are the data points from IceCube Collaboration (2014), while the open points are the  $3\sigma$  upper limits. The upper (magenta) short dashed lines represents the 90% C.L. upper limits from The Pierre Auger Collaboration (2015) while the lower (cyan) short dashed line is the expected three year sensitivity curve for the Askaryan Radio Array (Ara Collaboration 2012).

#### 4 THE NEUTRINO BACKGROUND FROM BL LACS

Fig. 1 shows our results, with different lines corresponding to different assumptions. Namely, and starting from the top:  $Y_{\nu\gamma}$  anti-correlated with  $L_\gamma (> 10 \text{ GeV})$  for all BL Lacs (black dot short-dashed line) and HBL (black dot long-dashed line);  $Y_{\nu\gamma} = 0.8$  and  $E_{\text{break}} = 200 \text{ GeV}$ ,  $\Delta\Gamma = 0.5$ , for all BL Lacs (blue solid line) and HBL (blue dotted line);  $Y_{\nu\gamma} = 0.8$  and  $E_{\text{break}} = 100 \text{ GeV}$ ,  $\Delta\Gamma = 1$ , for all BL Lacs (green long dashed line). The (red) filled circles are the data points from IceCube Collaboration (2014), while the open points are the  $3\sigma$  upper limits, derived from the  $1\sigma$  ones by simply scaling them by a factor  $\sim 3.6$  (Gehrels 1986). The upper (magenta) short dashed lines represents the 90% C.L. upper limits from The Pierre Auger Collaboration (2015) while the lower (cyan) short dashed line is the expected three year sensitivity curve for the Askaryan Radio Array (Ara Collaboration 2012).

A few points can be made about this figure:

- (i) BL Lacs as a class can easily explain the whole

NBG at high-energies ( $\gtrsim 0.5 \text{ PeV}$ ) while they do not contribute much ( $\sim 10\%$ ) at low-energies ( $\lesssim 0.5 \text{ PeV}$ );

(ii) HBL make up the bulk of the NBG in all cases up to  $\approx 30 \text{ PeV}$ , where they start to contribute less and less. This is where LBL take over, due to their lower  $\nu_{\text{peak}}^S$  and therefore larger values of neutrino peak energy, given the inverse dependence between  $\nu_{\text{peak}}^S$  and  $E_{\nu,p}$  (eq. 2). Note that HBL manage to dominate the neutrino output despite their small fraction ( $\sim 5\%$ ) because of their relatively high  $\gamma$ -ray, and therefore neutrino, fluxes and powers;

(iii) there is very little difference between the  $E_{\text{break}} = 200 \text{ GeV}$ ,  $\Delta\Gamma = 0.5$  and the  $E_{\text{break}} = 100 \text{ GeV}$ ,  $\Delta\Gamma = 1$  cases. This is due to the fact that we relate the neutrino flux to  $F_\gamma (> 10 \text{ GeV})$  and most of the  $\gamma$ -ray flux is at lower energies. Thus, the neutrino flux in the latter case is only slightly smaller than in the former;

(iv) The difference between the constant and varying  $Y_{\nu\gamma}$  case is small up to  $E_\nu \sim 1 - 2 \text{ PeV}$ . However, at  $E_\nu \gtrsim 5 \text{ PeV}$  only the constant  $Y_{\nu\gamma}$  case is fully consistent with the IceCube data, while the varying  $Y_{\nu\gamma}$  scenario is barely within the  $3\sigma$  upper limits. Moreover, current Auger upper limits already rule out our varying  $Y_{\nu\gamma}$  scenario, while future ones will better probe the high-energy tail. The Askaryan Radio Array, by sampling the  $\gtrsim 10 \text{ PeV}$  range with high sensitivity, will further constrain our model, together with the Antarctic Ross Ice Shelf Antenna Neutrino Array (ARIANNA, Barwick et al. 2015), which will cover the  $100 \text{ PeV} - 10 \text{ EeV}$  energy range;

(v) if our model is correct, IceCube should see more  $E_\nu > 1 \text{ PeV}$ , and even  $E_\nu > 2 \text{ PeV}$ , events; alternatively, a non-detection will put strong constraints on  $Y_{\nu\gamma}$  (see Sect. 5.5).

Given the above discussion, from now on we refer to the  $Y_{\nu\gamma} = 0.8$  and  $E_{\text{break}} = 200 \text{ GeV}$ ,  $\Delta\Gamma = 0.5$  case as our “benchmark” case.

Giommi & Padovani (2015) have shown that if the Monte Carlo simulations are modified to include the strong dependence of  $\nu_{\text{peak}}^S$  on radio power postulated by the blazar sequence (Fossati et al. 1998) the agreement with the observational data disappears, as the predicted  $\gamma$ -ray background above a few GeV turns out to be far in excess of the observed value. A similar thing happens for the predicted NBG, which, for example, turns out to be more than two orders of magnitude above the IceCube data at  $E_\nu \sim 1 \text{ PeV}$ .

Fig. 1 gives a feeling for the average NBG but not for the dispersion intrinsic to our simulation process. This is shown in Fig. 2, where the results from the ten different simulations are displayed individually. Different lines correspond to different assumptions. Namely, our benchmark case: average value (solid blue line) and individual runs (dotted blue lines);  $Y_{\nu\gamma} = 0.8$  and  $E_{\text{break}} = 100 \text{ GeV}$ ,  $\Delta\Gamma = 1$ : average value (long dashed green line) and individual runs (dot long-dashed green lines). The top line (cyan dot short-dashed line) represents the case with  $E_{\text{break}} = 200 \text{ GeV}$ ,  $\Delta\Gamma = 0.5$  but  $Y_{\nu\gamma} = 3$ . As this is the maximum value expected in our model for this parameter (e.g. Petropoulou & Mastichiadis 2015) this curve represents the largest NBG from BL Lacs. The black square is the neutrino flux of IceCube event 9 (Padovani & Resconi

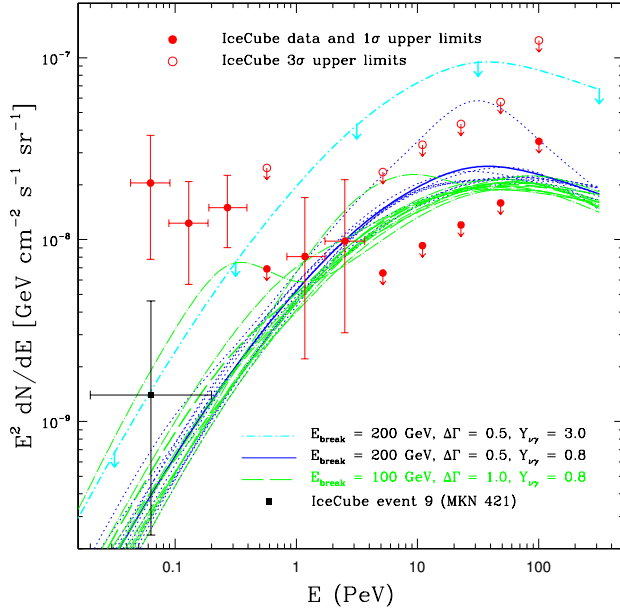


**Figure 2.** The predicted neutrino ( $\nu + \bar{\nu}$ ) background per neutrino flavour from BL Lacs for three different cases and showing the range of results from ten different simulations. Different lines correspond to different assumptions (starting from the top):  $Y_{\nu\gamma} = 3$  (the maximum theoretical value: cyan dot short-dashed line) and  $E_{\text{break}} = 200$  GeV,  $\Delta\Gamma = 0.5$ ;  $Y_{\nu\gamma} = 0.8$  and  $E_{\text{break}} = 200$  GeV,  $\Delta\Gamma = 0.5$ : average value (solid blue line) and individual runs (dotted blue lines);  $Y_{\nu\gamma} = 0.8$  and  $E_{\text{break}} = 100$  GeV,  $\Delta\Gamma = 1$ : average value (long dashed green line) and individual runs (dot long-dashed green lines). The (red) filled points are the data points from IceCube Collaboration (2014), while the open points are the  $3\sigma$  upper limits. The black square is the neutrino flux of IceCube event 9, from Padovani & Resconi (2014), who have tentatively associated it with MKN 421, converted to “background” units (i.e. divided by  $4\pi$ ).

2014) converted to “background” units (i.e. divided by  $4\pi$ ).

A few points can be made about this figure:

- (i) the dispersion amongst the ten different simulations for the two cases is typically not very large ( $\lesssim 0.3$  dex), with only 1 – 2 of them being clear outliers. In all cases this is due to a *single* source, which has a neutrino flux  $\sim 20 - 45$  times higher than the source with the second largest flux, at the energy where a “bump” can be seen in the curves. This has to be expected given the nature of the simulations but these outliers happen only  $\sim 10 - 20\%$  of the time;
- (ii) the presence of these outliers can explain at least some of the low-energy associations made by Padovani & Resconi (2014). The neutrino flux of IceCube event 9, which has been tentatively associated by these authors with MKN 421, is in fact fully compatible with one of the runs. Moreover, the number of events predicted by some of these outliers at low energies ( $E_\nu < 2$  PeV) is about twice as large as the mean of the ten simulations;
- (iii) the curve for the case with  $Y_{\nu\gamma} = 3$  defines the region of parameter space allowed by our model. At high

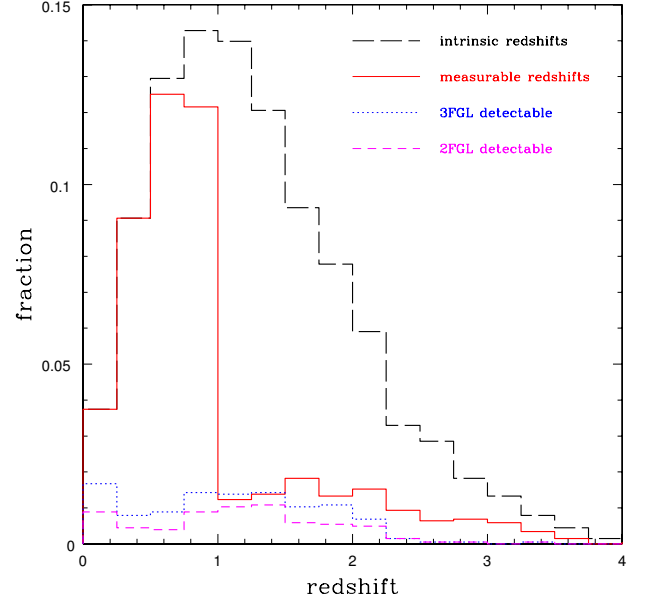


**Figure 3.** The redshift distribution for the BL Lacs contributing  $\sim 95\%$  of the background associated with the benchmark case at 1 PeV (black long-dashed line) and for those with a measurable redshift (red solid line). The sources detectable by the 3FGL (blue dotted line) and 2FGL (magenta short-dashed line) catalogues are also indicated.

energies this is well above the IceCube  $3\sigma$  upper limits, which means that this upper bound is clearly ruled out by current data, and therefore that a leptonic component must be present in the  $\gamma$ -ray emission of blazars.

## 5 DISCUSSION

### 5.1 Characterising the NBG sources

As is normally the case for astrophysical backgrounds, most of the NBG is produced by a small fraction of the population. In our case,  $\sim 0.5\%$  of the BL Lacs make  $\sim 95\%$  of the background associated with the benchmark case at 1 PeV, which is where our predictions are quite close to the IceCube data. We now focus on this sub-sample and describe some of its properties.

Fig. 3 shows the redshift distributions for the whole sub-sample<sup>7</sup> (dashed line) and for the subset of BL Lacs with measurable redshift (red solid line). Note that the latter make up  $\sim 50\%$  of the sub-sample, with the other 50% consisting of BL Lacs with *no* measurable redshift. These are BL Lacs whose maximum equivalent width (EW) is  $\lesssim 2$  Å, or for which the non-thermal light is at least a factor 10 larger than that of the host galaxy, and are therefore deemed to have a redshift which cannot be typically measured (Paper I). As expected, the two distributions are quite different with  $\langle z \rangle \sim 1.3$  and  $\sim 0.9$  respectively. This is due to the fact that the sources with

<sup>7</sup> We note that this is not significantly different from the redshift distribution of the entire sample.

no measurable redshift are mostly those with the optical spectra swamped by non-thermal emission, which tend to have a more powerful jet and therefore are on average at larger intrinsic redshift.

The fraction of sources in the sub-sample detectable by the 3FGL *Fermi* catalogue (The Fermi-LAT Collaboration 2015) is  $\sim 11\%$ . However, these make  $\sim 50\%$  of the overall background associated with the benchmark case, i.e.  $\sim 15\%$  of the NBG. We also find that  $\sim 7\%$  of the sources would be detectable by the 2FGL (Nolan et al. 2012), making  $\sim 40\%$  of the background associated with the benchmark case, i.e.  $\sim 12\%$  of the NBG. These numbers are consistent with the preliminary results of Glüsenkamp et al. (2015), who find no evidence of neutrino emission and a maximal contribution from *Fermi* 2LAC (Ackermann et al. 2011) blazars  $\sim 20\%^8$ .

The (intrinsic) redshift distributions of the sources detectable by the 3FGL (blue dotted line) and 2FGL (magenta short-dashed line) catalogues are also shown in Fig. 3.

## 5.2 Possible caveats

### 5.2.1 LBL

The inclusion of the hadronic “prior” into the Monte Carlo simulations is based upon the results derived from individual SED fitting of HBL (Petropoulou et al. 2015). The application of our model to LBL, therefore, could not be straightforward. Thus, we discuss here possible caveats.

A direct application of eq. 2 to LBL requires that: (1) the photons of the low energy SED component are the main targets for photopion interactions; (2) acceleration of protons to ultra-high energies (UHE), e.g.  $10^{19} - 10^{20}$  eV, takes place in the jets of these sources. These assumptions, in turn, suggest that specific conditions should prevail in the emitting region of individual LBL, in order to explain their  $\gamma$ -ray emission in terms of photo-hadronic processes. In particular, if the  $\gamma$ -ray emission is synchrotron radiation of UHE secondary pairs (similarly to HBL), then the emitting region should contain very weak magnetic fields, e.g.  $B \ll 3\mu\text{G}$  (see also eq. 9 in Petropoulou & Mastichiadis 2015). Alternatively, the  $\gamma$ -ray emission of LBL could be the result of a hadronic cascade (Mannheim et al. 1991; Mannheim & Biermann 1992). If the above conditions can be realised in the jets of LBL, then application of eq. 2 shows that the LBL contribution to the NBG takes place at high energies, i.e.  $> 100$  PeV (see Fig. 1).

One could relax, however, assumption (2), if the targets for the photopion interactions were synchrotron photons with frequencies above  $\nu_{\text{peak}}^S = 10^{13}$  Hz (see generic SED in Fig. 8 in Petropoulou & Mastichiadis 2015). In this case, application of eq. 2 to LBL would also result in the production of neutrinos with energies similar to those expected from HBL<sup>9</sup>. In this scenario, the neutrino

emission from both HBL and LBL sources is expected to have a similar peak energy.

To test the robustness of the results shown in Figs. 1 and 2 we therefore artificially shifted the  $\nu_{\text{peak}}^S$  distribution of LBL so that it had the same mean as HBL, using the same value of  $Y_{\nu\gamma}$ . We then repeated the Monte Carlo simulations and found that the total NBG flux increased only by  $\simeq 15\%$  overall. This is due to the fact that LBL have much smaller  $\gamma$ -ray, and therefore neutrino, fluxes than HBL. It then follows that our results on the NBG do not depend on a detailed modelling of LBL and are therefore robust.

### 5.2.2 Energetics

Leptohadronic models are known to predict relatively high jet powers, driven by their relativistic proton content (e.g. Zdziarski & Böttcher 2015; Petropoulou et al. 2015, and references therein). Indeed, the estimated jet power for the six HBL to which Petropoulou et al. (2015) applied their leptohadronic model, and which lie at the basis of our calculations, is quite high ( $L_{\text{jet}} \sim 2 \times 10^{48} - 8 \times 10^{49}$  erg s<sup>-1</sup> [see their Tab. 4]).

One could compare  $L_{\text{jet}}$  with the Eddington luminosity,  $L_{\text{Edd}}$ , of those sources. Assuming a typical black hole mass of  $3 \times 10^8 M_{\odot}$  (Plotkin et al. 2011), this would be  $\sim 3.8 \times 10^{46}$  erg s<sup>-1</sup>, which, in turn, would imply that the jet power is  $\gtrsim 50$  (and up to  $\sim 2,000$ ) times larger. These large  $L_{\text{jet}}/L_{\text{Edd}}$  ratios are not necessarily alarming, for the following reasons: 1. out of the six BL Lacs modelled in Petropoulou et al. (2015) only for MKN 421 is there an estimate for the black hole mass (Sbarrato et al. 2012) (which happens to be equal to the value we have assumed), which means that a comparison against an uncertain  $L_{\text{Edd}}$  is not very informative; 2. Ghisellini et al. (2014), by applying a *leptonic* model to a large sample of mostly FSRQ, have derived at low powers  $L_{\text{jet}} \approx L_{\text{Edd}}$ , with some sources reaching  $L_{\text{jet}}/L_{\text{Edd}} \approx 30$ . At least some of the sources studied by Petropoulou et al. (2015) (including MKN 421) lie close to the upper range of that distribution; 3. the total jet power does not need to be limited by  $L_{\text{Edd}}$ , as is observed, for example, in the case of gamma-ray bursts, which are super-Eddington by huge amounts ( $\approx 10^{10}$ ; e.g. Piran 2004).

A more meaningful comparison would be that of  $L_{\text{jet}}$  with  $\dot{M}c^2$ , where  $\dot{M}$  is the accretion rate. One in fact expects  $L_{\text{jet}} \sim \epsilon_j \dot{M}c^2$  with  $\epsilon_j \lesssim 1.5$  (Zdziarski & Böttcher 2015, and references therein). In the case of radiatively efficient accretors, the accretion rate is normally derived from the relation  $\dot{M}c^2 = L_{\text{disk}}/\eta$ , where  $\eta$  is the radiative efficiency.  $L_{\text{disk}}$ , in turn, is estimated through the broad emission lines, which are used, via a template, to derive the luminosity of the entire broad line region ( $L_{\text{BLR}}$ ). The latter is therefore a proxy for the accretion disk luminosity, modulo a covering factor, which is usually taken to be  $\sim 0.1$  (which means  $L_{\text{disk}} \sim 10L_{\text{BLR}}$ ; Ghisellini et al. 2014, and references therein). None of the six sources studied by Petropoulou et al. (2015) shows broad lines, while only two sources display narrow lines in their spectra. In fact, our sources are most likely LERGs and therefore radiatively inefficient accretors. In short, it is not

<sup>8</sup> This is however derived assuming an  $E^{-2.46}$  spectrum, which is much softer than our predictions.

<sup>9</sup> A preliminary application to Ap Librae results in  $Y_{\nu\gamma} \sim 0.5$  and a neutrino peak energy of several PeV.

possible to derive the accretion power of these sources, since they do not exhibit broad line features. Most importantly though, we could not relate  $L_{\text{disk}}$  to  $\dot{M}c^2$  because the simple relation, which is valid for radiatively efficient accretors, breaks down for LERGs (Sbarrato, Padovani, & Ghisellini 2014, and references therein). The point remains that we do not expect high values of  $\dot{M}$ , as otherwise these sources could not be LERGs.

If our model will be confirmed by future IceCube detections, this will simply mean that the current picture of accretion in broad-lined, efficient accretor AGN cannot be applied to HBL.

As a final point, we note that the energetics for BL Lacs in the proton synchrotron scenario are more reasonable than in the leptohadronic one (Dimitrakoudis, Petropoulou, & Mastichiadis 2014) but in that case the neutrino flux from BL Lacs would peak at  $E_\nu \sim 200$  PeV and would be much lower than in our model.

It could be argued that, given the high powers in relativistic protons, proton-proton ( $pp$ ) collisions with the background (thermal) protons in the inner jets of blazars could result in a substantial production of neutrinos. While a detailed study of this process goes beyond the scope of this paper, we note that, having a neutrino flux from the  $pp$  mechanism equal to that from the  $p\pi$  interaction at  $\sim 1$  PeV, would require thermal proton number densities  $\approx 10^8 \text{ cm}^{-3}$ . These, in turn, would translate into a (thermal) proton energy density  $\sim 1 - 2$  orders of magnitude larger than that derived by Petropoulou et al. (2015) and a correspondingly larger  $L_{\text{jet}}$ . We thus contend that this scenario is not plausible (see also Atoyan & Dermer 2003).

### 5.2.3 FSRQ

The model we used for including neutrino emission in the Monte Carlo simulation has not been applied to FSRQ, which we therefore excluded from our calculations. A proper treatment of the neutrino emission from individual FSRQ is required in order to make robust predictions about their cumulative contribution, but this lies outside the scope of the present study. Recently, Dermer, Murase, & Inoue (2014) and Murase, Inoue & Dermer (2014) have calculated the neutrino background from FSRQ based on the blazar sequence and assuming a leptonic origin of the blazar  $\gamma$ -ray emission. They have taken into account photopion interactions with the non-thermal emission from the jet and the external photon fields (BLR and dusty torus). The latter have been shown to provide most of the contribution to the total neutrino output.

Here instead, we calculated the NBG from FSRQ assuming that they fall within the same scenario of BL Lacs, an assumption that has no astrophysical basis. We find that their contribution to the NBG is somewhat energy dependent but overall only  $\approx 30\%$  that of BL Lacs. We caution the reader that this estimate neglects the role of external photon fields in the photopion interactions and, therefore, in the final neutrino output. As such, this contribution should be considered as a lower limit.

### 5.2.4 Masquerading BL Lacs

Paper I and II discussed the existence of sources, which appeared “BL Lac-like” only because their emission lines were heavily diluted by strong non-thermal emission. These objects, which are therefore “masquerading” BL Lacs and are in fact misclassified FSRQ, make up a very small fraction ( $\sim 2\%$ ) of our BL Lacs. However, as is the case for HBL, because of their relatively high  $\gamma$ -ray, and therefore, neutrino fluxes, their contribution to the NBG is  $\approx 60\%$  that of all BL Lacs. Our calculations on the neutrino emission were made under the assumption that only photons produced internally in the jet, i.e. synchrotron photons, are the targets for photopion interactions. In masquerading BL Lacs any line- or blackbody-like emission external to the jet is hidden below the non-thermal synchrotron emission that is produced within the jet. We argue that our model is also applicable to these sources, as long as  $u'_{\text{syn}} \gtrsim u'_{\text{ex}}$ , where  $u'_{\text{syn}}$  and  $u'_{\text{ex}} \simeq \Gamma^2 u_{\text{ex}}$  (where  $\Gamma$  is the Lorentz factor) are the energy densities of synchrotron and external photons, respectively, as measured in the rest-frame of the emitting region. Obviously, our argument becomes even stronger if the boosting of the external energy density becomes less efficient (e.g. the non-thermal emitting region is located much further out than the external photon field region).

### 5.2.5 Flaring sources

One of the defining characteristics of blazars is their large variability known to occur in all parts of the electromagnetic spectrum. The specific amount depends on the energy band and on the blazar type, with values ranging from a factor of a few in the radio band up to a factor 10,000 at GeV energies (e.g. Aharonian et al. 2007; Giommi 2015). The amount of variability of the neutrino flux in blazars and how this correlates with  $\gamma$ -ray variability is not known. As the number of astrophysical neutrino events detected so far is still very small, one could speculate that large flaring events from one or a few of the brighter sources in Fig. 2 may produce a fair fraction of the observed events. This is not straightforward though, and requires detailed modelling of flaring sources (e.g. Reimer et al. 2005). A more recent application to the flaring MKN 421 also suggests that an accumulation of flaring events from an individual source may be needed in order to have a statistically significant neutrino detection (Petropoulou et al., in preparation). Here we consider the emission arising from the entire population of BL Lacs and assume that flares from single sources will be diluted by the integrated emission from all blazars.

## 5.3 Comparison with previous results

The idea of blazars being sources of high-energy neutrinos dates back to long before the detection of sub-PeV neutrinos with IceCube (IceCube Collaboration 2013) and has since been explored in a number of studies (e.g. Mannheim 1995; Halzen & Zas 1997; Mücke et al. 2003; Tavecchio & Ghisellini 2015; Kistler, Stanev, & Yüksel 2014; Dermer, Murase, & Inoue 2014; Murase, Inoue &



Dermer 2014). Our approach has some similarities but many differences with previous work, as detailed below.

### 5.3.1 Similarities

- (i) the BL Lac  $\gamma$ -ray emission has a (photo)hadronic origin (at least for the models presented in Fig. 4);
- (ii) in BL Lacs the targets for photopion interactions are the low-energy synchrotron photons.

### 5.3.2 Differences

(i) we use as a starting point the knowledge gained from detailed SED fitting of BL Lacs instead of using a generic neutrino spectrum (e.g. Mannheim, Protheroe & Rachen 2001; Kistler, Stanev, & Yüksel 2014; Murase, Inoue & Dermer 2014). By establishing a connection between the  $\gamma$ -ray and neutrino emission for each source (see eqs. 2 – 5), we are able to assign to *each* simulated BL Lac in the Monte Carlo code a unique neutrino spectrum. We then calculate the NBG by summing up the fluxes of all sources in each energy bin;

(ii) for the calculation of the NBG we do not normalise *a priori* a generic neutrino spectrum to the extragalactic  $\gamma$ -ray background (EGB) (e.g. Mannheim 1995; Mücke et al. 2003). In fact, we do not need to, as our simulation naturally reproduces the observed EGB above 10 GeV (Giommi & Padovani 2015);

(iii) the NBG spectrum is not *a priori* normalised to the IceCube observations (e.g. Tavecchio & Ghisellini 2015). Instead, for a specific choice of  $Y_{\nu\gamma}$ , which is the only tuneable parameter in our framework, we compare our model predictions with the IceCube data;

(iv) the maximum proton energy is taken to be a few times larger than the threshold energy for photopion interactions with the peak energy synchrotron photons of the low-energy hump. This is usually lower than the values used in previous studies (e.g. Halzen & Zas 1997; Mücke et al. 2003), which also explains the difference in the peak energies of the NBG;

(v) the  $\gamma$ -ray emission of individual BL Lacs in our approach is a combination of synchrotron radiation emitted by electron-positron pairs produced through  $\pi^\pm$  decay and synchrotron self-Compton from primary electrons. The cascade emission initiated by  $\pi^0$   $\gamma$ -rays has a negligible effect in the formation of the blazar SED. This is in contrast to previous studies, where the blazar  $\gamma$ -ray emission is explained either as proton synchrotron radiation (e.g. Mücke et al. 2003) or as cascade emission (e.g. Halzen & Zas 1997; Kistler, Stanev, & Yüksel 2014).

### 5.3.3 Detailed comparison

Fig. 4 compares the predicted neutrino background for our benchmark case for all BL Lacs (blue solid line) and HBL (blue dotted line) with some of the previous results. In chronological order, these are: Mannheim (1995) (long dashed cyan line, upper limits at low energies), Halzen & Zas (1997) (short dashed green line), Mücke et al. (2003) (dot long-dashed black lines), and Tavecchio & Ghisellini (2015) (dot short-dashed magenta line). The two curves

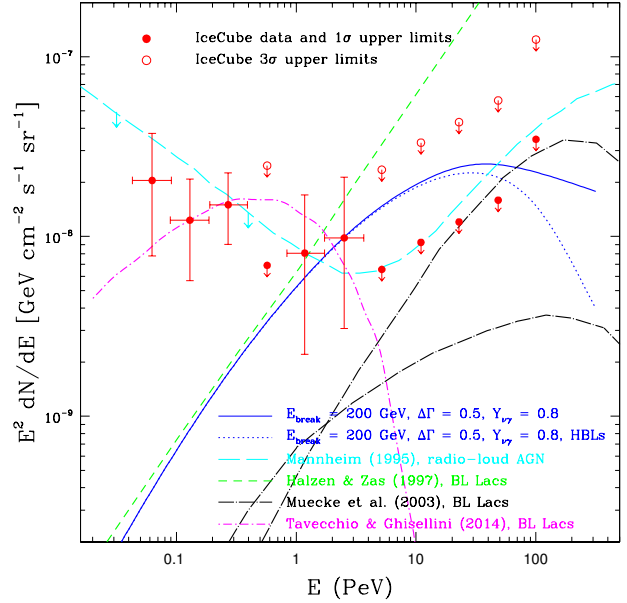


**Figure 4.** The predicted neutrino background per neutrino flavour for  $Y_{\nu\gamma} = 0.8$  and  $E_{\text{break}} = 200$  GeV,  $\Delta\Gamma = 0.5$ , for all BL Lacs (blue solid line) and HBL (blue dotted line) compared to previous results. Namely, in chronological order: Mannheim (1995) (long dashed cyan line; upper limits at low energies), Halzen & Zas (1997) (short dashed green line), Mücke et al. (2003) (dot long-dashed black lines: LBL, upper curve; HBL, lower curve), and Tavecchio & Ghisellini (2015) (dot short-dashed magenta line). The (red) filled points are the data points from IceCube Collaboration (2014), while the open points are the  $3\sigma$  upper limits. See text for details.

from Mücke et al. (2003) represent the *maximum* contribution expected from LBL (upper curve) and HBL (lower curve), respectively. A few things about Fig. 4 are worth mentioning:

(i) the model by Mannheim (1995) at first glance is the one that best describes the IceCube data. This, taken at face value, would imply that radio-loud AGN explain the entire NBG, something that contradicts the preliminary IceCube results of Glusenkamp et al. (2015), who find a maximal contribution from *Fermi* 2LAC (Ackermann et al. 2011) blazars  $\sim 20\%$ . However, since it gives only upper limits at low energies, it could be still reconciled with the data. This model has a very different shape as compared to the others because it includes *two* hadronic components, i.e. a low-energy soft one ( $E_\nu \lesssim 2$  PeV), produced through  $pp$  collisions of the escaping CRs from the blazar jet with the ambient medium, and a high-energy flat one ( $E_\nu \gtrsim 2$  PeV), related to  $p\pi$  interactions of CRs with the synchrotron photons in the blazar jet;

(ii) the model by Halzen & Zas (1997), although very close to ours at low energies, lies above the  $3\sigma$  upper limits at  $E_\nu \gtrsim 5$  PeV, while the sum of the two curves by Mücke et al. (2003) remains consistently below the IceCube data. Although the model curve of Tavecchio & Ghisellini (2015) passes through the data points, this is by construction, i.e. the NBG was *a priori* normalised to the IceCube data. Moreover, this model might also con-

tradict the IceCube results of Glüsenkamp et al. (2015) mentioned above (pending the different spectral shapes);

(iii) apart from the Tavecchio & Ghisellini (2015) model and the low-energy ( $E_\nu < 2$  PeV) part of the Mannheim (1995) model, the NBG spectrum below its peak is relatively hard in all other models shown in Fig. 4. This is related to the assumed proton power-law index and the spectrum of target photons, which are both similar among the models. The diversity of the peak energy of the NBG spectrum, on the other hand, reflects mainly the different model assumptions on the maximum proton energy in blazars.

#### 5.4 Cosmic rays

Neutrons that are produced in photopion interactions are an effective means of CR escape from the system. They are unaffected by its magnetic field, their decay time is high enough to allow them to escape freely before reverting into protons (Kirk & Mastichiadis 1989; Begelman, Rudak, & Sikora 1990; Giovanoni & Kazanas 1990; Atoyan & Dermer 2003), and they are unaffected by adiabatic energy losses that the protons may sustain in the system as it expands (Rachen & Mészáros 1998). For the purposes of this paper, we will assume that “neutron conversion” is the injection mechanism of CRs from BL Lacs into the intergalactic medium (e.g. Kistler, Stanev, & Yüksel 2014), while we neglect any additional contribution to the neutrino and CR fluxes from direct proton escape (e.g. Essey et al. 2010; Kalashev, Kusenko, & Essey 2013). This is a valid assumption as long as the escaping protons are susceptible to adiabatic energy losses (e.g. the emitting region lies within an expanding jet) (Rachen & Mészáros 1998) and may end up carrying a negligible fraction of the UHECR flux. In this regard, the CR flux estimates that follow should be considered as a lower limit.

The neutron spectrum, and thus, the escaping CR spectrum from each BL Lac, can be directly related to the neutrino spectrum (see e.g. Fig. 9 in Dimitrakoudis et al. 2012), at least in the optically thin regime for  $p\pi$  interactions<sup>10</sup>. Under certain simplifying assumptions, namely: (1)  $E_n \simeq 20E_\nu$ ; (2)  $E_p \simeq E_n$ ; and (3) production of one  $\pi^\pm$  pair per interaction, which leads to  $E_n dN/dE_n \approx (1/6)E_\nu dN/dE_\nu$  (see also Kistler, Stanev, & Yüksel 2014), we may write

$$E_p^2 \frac{dN}{dE_p} \approx \frac{20}{6} E_\nu^2 \frac{dN}{dE_\nu}. \quad (6)$$

Having already calculated the NBG flux in Sect. 4, we can easily apply the above relation to all BL Lacs and estimate their contribution to the injected CR spectrum without taking into account any propagation effects. This will be a “copy” of the total NBG spectrum shown in Figs. 1 and 2, translated to higher energies by a factor of  $\sim 20$  and scaled in flux by a factor<sup>11</sup> of 10.

<sup>10</sup> The BL Lac emitting region is optically thin to  $p\pi$  interactions with typical optical depths  $\tau_{p\pi} \sim 10^{-6} - 10^{-4}$  (see e.g. Atoyan & Dermer 2001; Petropoulou et al. 2015).

<sup>11</sup> Equation 6 was derived taking into account neutrinos of

The resulting CR spectrum from HBL for our benchmark case peaks at  $E_p \sim 2.5 \times 10^{18}$  eV with a flux  $\sim 3.0 \times 10^{24}$  eV<sup>2</sup> m<sup>-2</sup> s<sup>-1</sup> sr<sup>-1</sup>, only slightly above the observational data (see High Resolution Fly’S Eye Collaboration et al. 2009; Abu-Zayyad et al. 2013; The Pierre Auger Collaboration 2013). A proper comparison would require the calculation of the expected proton fluxes at Earth taking into account propagation effects. Namely: (i) photopion (e.g. Mücke et al. 1999) and photopair (Blumenthal 1970) production on the background photon fields (cosmic microwave, cosmic infrared, and cosmic optical backgrounds); (ii) adiabatic energy losses; and (iii) magnetic deflections due to the intergalactic magnetic field.

From the above, it becomes evident that a detailed treatment of LBL is also required, since the specifics of their SED modelling (e.g. the maximum proton energy) will affect our predictions of the UHECR spectrum. We plan to calculate the CR flux predicted by our scenario in detail in a future paper.

#### 5.5 Model predictions

Our model makes specific predictions on the detectability of  $E_\nu > 2$  PeV events, that is above the current maximum energy of IceCube neutrinos. We have used the effective areas from IceCube Collaboration (2013) and our NBG to predict the number of  $2 < E_\nu < 10$  PeV neutrino events IceCube should see (as 10 PeV is the maximum energy for which IceCube effective areas are available). We get  $N_\nu \sim 4.6$  events for our benchmark case assuming the Glashow resonance (Glashow 1960) is not relevant since we are dealing with proton-photon interaction (Anchordoqui et al. 2005) (and  $N_\nu \sim 7$  otherwise). For our other case ( $Y_{\nu\gamma} = 0.8$  and  $E_{\text{break}} = 100$  GeV,  $\Delta\Gamma = 1.0$ ) we derive  $N_\nu \sim 4.0$  (or 6.1) events. Since the NBG of our models peak at  $E_\nu > 10$  PeV by making an educated guess on the effective areas we estimate an additional 2–3 events up to  $\sim 100$  PeV. Noting that the  $3\sigma$  upper limit for 0 events is 6.6 (Gehrels 1986), we are actually close to being inconsistent with the IceCube non-detections. However, our number is probably biased because  $Y_{\nu\gamma} = 0.8$  is likely an upper limit. This was derived, in fact, from a small sample of BL Lacs, which might represent the tip of the iceberg in terms of neutrino emission, as they were selected as the most probable candidates. For example, if  $Y_{\nu\gamma} = 0.3$  then for our benchmark case  $N_\nu \approx 3$  (4) for  $2 < E_\nu < 100$  PeV, which is well within the  $2\sigma$  limit for 0 events. In any case, our predictions should easily be testable by IceCube in the next few years.

Turning things around, we showed that the shape and the peak energy of the neutrino spectrum expected from a single BL Lac are mostly determined by its low-energy emission and the Doppler factor of the source (see Sect. 3.1). Thus, the calculation of the diffuse neutrino emission from BL Lacs can be considered to be robust. Most importantly though, our method has only one tuneable parameter, namely the ratio  $Y_{\nu\gamma}$  (eq. 5). A com-

all-flavours, whereas the NBG flux shown in Figs. 1 and 2 is per neutrino flavour.

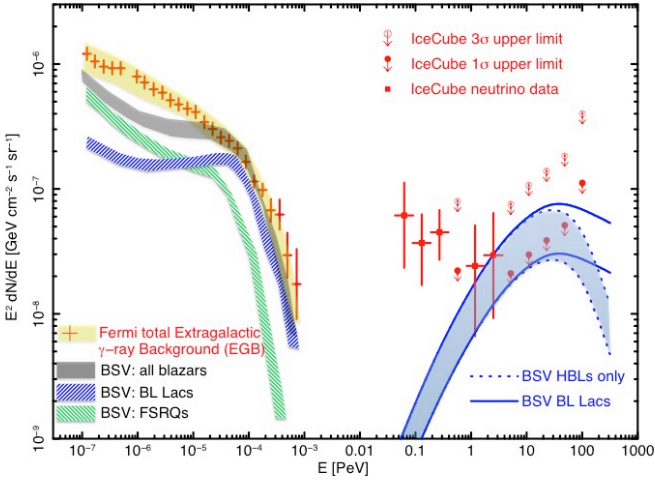


**Figure 5.** The electromagnetic and neutrino extragalactic backgrounds predicted by our simulations in the energy range 100 MeV – 300 PeV. The left side of the plot ( $E < 1$  TeV) shows the  $\gamma$ -ray background for various classes compared to the total extragalactic electromagnetic emission observed by *Fermi*-LAT (adapted from Paper IV), whereas the right side ( $E > 10$  TeV) illustrates our prediction for the neutrino background (all flavours) for our benchmark case ( $E_{\text{break}} = 200$  GeV,  $\Delta\Gamma = 0.5$ ) for all BL Lacs (blue solid line) and HBL (blue dotted line) and  $Y_{\nu\gamma}$  ranging between 0.8 (upper curves) and 0.3 (lower curves; see text for details). The (red) filled points are the (all flavours) data points from IceCube Collaboration (2014), while the open points are the  $3\sigma$  upper limits.

parison of the model predicted NBG with current IceCube upper limits and, ultimately, future detections at  $E_\nu > 2$  PeV, can be used to constrain the value of  $Y_{\nu\gamma}$ . In other words, this would provide an indirect way of probing the origin of the BL Lac  $\gamma$ -ray emission.

## 5.6 The big picture

Fig. 5 displays both the electromagnetic and neutrino extragalactic backgrounds predicted by our simulations and the available measurements in the energy range 100 MeV – 300 PeV. The left side shows the  $\gamma$ -ray background compared to the total extragalactic electromagnetic emission observed by *Fermi*-LAT (adapted from Paper IV), whereas the right side illustrates our prediction for the NBG (all flavours) for our benchmark case for all BL Lacs (blue solid line) and HBL (blue dotted line) and  $Y_{\nu\gamma}$  ranging between 0.8 (upper curves) and 0.3 (lower curves), the latter value being more consistent with the IceCube high-energy non-detections.

The EGB can be approximated by a power law with exponential cutoff having  $\Gamma \simeq 2.3$  and a break energy  $\sim 280$  GeV (Ackermann et al. 2015), the latter very likely due to the EBL absorption of  $\gamma$ -ray photons from distant ( $z \gtrsim 0.3$ ) sources (e.g. Ajello et al. 2015, and Paper IV). As a simple extrapolation of the EGB power law to the PeV energy range goes through the IceCube data, it might be tempting to assume that there is a single class

of sources that explains both the EGB at  $E \lesssim 10$  GeV and the NBG below  $\sim 0.5$  PeV. This population cannot be the blazar one, for the following two reasons: (i) in the BSV scenario, blazars contribute  $\sim 50\% - 70\%$  to the total EGB at  $E \lesssim 10$  GeV, while BL Lacs may explain almost 100% of the EGB flux at  $E \gtrsim 100$  GeV; (ii) similarly, BL Lacs contribute only  $\sim 10\%$  to the NBG at energies  $< 0.5$  PeV, while they may fully explain the observed NBG above 0.5 PeV. If starburst galaxies can explain part of the EGB at  $E > 100$  MeV (e.g. Lacki, Horiuchi, & Beacom 2014, and references therein) then they could also be a promising candidate class for explaining the sub-PeV IceCube neutrinos (e.g. Loeb & Waxman 2006; Stecker 2007). We note, in fact, that in proton-proton scenarios of  $\gamma$ -ray emission, relevant to starburst galaxies, the neutrino and  $\gamma$ -ray spectra have the same power law index as the parent proton population (e.g. Kelner, Aharonian, & Bugayov 2006).

Alternatively (or at the same time) the low-energy neutrino events could also have a Galactic component (e.g. Padovani & Resconi 2014). In any case, if there is a different class of sources contributing to the sub-PeV energy range, there is still room for individual BL Lac sources, like MKN 421 (see Fig. 2 and relevant discussion). Finally, we note that the EGB in Fig. 5 shows the sum of unresolved and resolved  $\gamma$ -ray emission of the extragalactic sky, whereas in the case of IceCube neutrinos we are not yet in the position to distinguish between a resolved and an unresolved contribution. The current status of neutrino astronomy, therefore, somewhat resembles that of  $\gamma$ -ray astronomy in its very early days (i.e. those of SAS-2 and COS-B).

The scenario, which appears to emerge by comparing our model NBG with the data is the following: at low energy ( $E_\nu \lesssim 0.5$  PeV) BL Lacs can only explain  $\sim 10\%$  of the IceCube data. Some other population/physical mechanism needs to provide the bulk of the neutrinos. However, this does not exclude the possibility that individual BL Lacs still make a contribution at the  $\approx 20\%$  level to the IceCube events. At high energy ( $E_\nu \gtrsim 0.5$  PeV) BL Lacs can account fully for the IceCube data. The strong implications of our scenario are: 1. IceCube should soon start resolving at least some of the NBG; 2. IceCube should also detect events at  $E_\nu \gtrsim 2$  PeV in the next few years.

## 6 CONCLUSIONS

We have included in the *blazar simplified view* scenario, which reproduces extremely well the statistical properties of blazars from the radio to the  $\gamma$ -ray band, a hadronic component and calculated via a leptohadronic model the neutrino background produced by the whole BL Lac class. For the first time, this is done by summing up the fluxes of all the BL Lacs generated by a Monte Carlo simulation, each with its own different properties. Our main results can be summarised as follows:

- (1) BL Lacs as a class can easily explain the whole neutrino background at high-energies ( $\gtrsim 0.5$  PeV) while

they do not contribute much ( $\sim 10\%$ ) at low-energies ( $\lesssim 0.5$  PeV).

(2) Individual BL Lacs, however, including some of the sources selected as possibly associated with some IceCube events by Padovani & Resconi (2014), can still make a contribution at the  $\approx 20\%$  level to the low-energy events.

(3) Given our Monte Carlo approach, we can easily characterise the BL Lacs producing most of the neutrino background. These are of the HBL type (up to  $E_\nu \approx 30$  PeV), have relatively low redshifts ( $\langle z \rangle \sim 1.3$ ), and about half of them have their optical spectra swamped by non-thermal emission and therefore an unmeasurable redshift. The (small) fraction of *Fermi* detectable sources in our scenario is consistent with a preliminary IceCube likelihood analysis on *Fermi* blazars.

(4) A simultaneous look at the  $\gamma$ -ray and neutrino backgrounds leads us to suggest that another population/physical mechanism could explain both the former at  $E \lesssim 10$  GeV (since blazars dominate above that energy) and the latter at  $E_\nu \lesssim 0.5$  GeV. This might include star forming galaxies, although a Galactic component for the low-energy IceCube events could also be possible.

(5) Our simulations at face value predict that IceCube should soon start resolving a fraction of the neutrino background and detect events at  $E_\nu > 2$  PeV. A non-detection will constrain the value of our only tuneable parameter ( $Y_{\nu\gamma}$ ) and will provide an indirect way of probing the origin of  $\gamma$ -ray emission in BL Lacs.

## ACKNOWLEDGMENTS

We thank Stefan Coenders, Gabriele Ghisellini, Tullia Sbarrato, and an anonymous referee, for useful comments. Support for this work was provided by NASA to MP through Einstein Postdoctoral Fellowship grant number PF3 140113 awarded by the Chandra X-ray Center, which is operated by the Smithsonian Astrophysical Observatory for NASA under contract NAS8-03060. ER is supported by a Heisenberg Professorship of the Deutsche Forschungsgemeinschaft (DFG RE 2262/4-1).

## REFERENCES

Aartsen M. G., et al., 2015, *Phys. Rev. Lett.*, 114, 171102  
 Abu-Zayyad T., et al., 2013, *ApJ*, 777, 88  
 Ackermann M., et al., 2011, *ApJ*, 743, 171  
 Ackermann M., et al., 2015, *ApJ*, 799, 86  
 Aharonian F. A., 2000, *New Astronomy*, 5, 377  
 Aharonian, F. A., et al. 2007, *ApJL*, 664, 71  
 Ahlers M., Halzen F., 2012, *Phys. Rev. D*, 86, 083010  
 Ajello M., et al., 2015, *ApJ*, 800, L27  
 Anchordoqui L. A., Goldberg H., Halzen F., Weiler T. J., 2005, *Phys. Letters B*, 621, 18  
 Ara Collaboration, 2012, *Astroparticle Physics*, 35, 457  
 Arsioli B., Fraga B., Giommi P., Padovani P., Marrese, M., 2015, *A&A*, 579, A34  
 Atoyan A. M., Dermer C. D., 2001, *Phys. Rev. Lett.*, 87, 221102  
 Atoyan A. M., Dermer C. D., 2003, *ApJ*, 586, 79

The Pierre Auger Collaboration, 2013, Contributions to the 33rd International Cosmic Ray Conference (ICRC 2013) (arXiv:1307.5059)  
 The Pierre Auger Collaboration, 2015, submitted to *Phys. Rev. D* (arXiv:1504.05397)  
 Barwick S. W., et al., 2015, *Astroparticle Physics*, 70, 12  
 M. C. Begelman, B. Rudak, M. Sikora, 1990, *ApJ*, 362, 38  
 Biermann P. L., Strittmatter P. A., 1987, *ApJ*, 322, 643  
 Blandford R. D., Rees M. J., 1978, in *Pittsburg Conference on BL Lac Objects*, Ed. A. M. Wolfe, Pittsburgh, University of Pittsburgh press, p. 328  
 Blumenthal G. R., 1970, *Phys. Rev. D*, 1, 1596  
 Dermer C. D., Ramirez-Ruiz E., Le T., 2007, *ApJ*, 664, L67  
 Dermer C. D., Murase K., Inoue Y., 2014, *Journal of High Energy Astrophysics*, 3, 29  
 Dimitrakoudis S., Mastichiadis A., Protheroe R. J., Reimer A., 2012, *A&A*, 546, AA120  
 Dimitrakoudis S., Petropoulou M., Mastichiadis A., 2014, *Astroparticle Physics*, 54, 61  
 Domínguez A., et al., 2011, *MNRAS*, 410, 2556  
 Essey W., Kalashev O. E., Kusenko A., Beacom J. F., 2010, *Phys. Rev. Lett.*, 104, 141102  
 The Fermi-LAT Collaboration, 2015, *ApJS*, in press (arXiv:1501.02003)  
 Fossati et al., 1998 *MNRAS*, 299, 433  
 Gehrels N. 1986, *ApJ*, 303, 336  
 Ghisellini G., Tavecchio F., Maraschi L., Celotti A., Sbarrato T., 2014, *Nature*, 515, 376  
 Giommi P., Padovani P., Polenta G., Turriziani S., D'Elia V., Piranomonte S., 2012a, *MNRAS*, 420, 2899 (Paper I)  
 Giommi P., et al., 2012b, *A&A*, 514, 160  
 Giommi P., Padovani P., Polenta G., 2013, *MNRAS*, 431, 1914 (Paper II)  
 Giommi P., 2015, *Journal of High Energy Astrophysics*, submitted (arXiv:1503.04863)  
 Giommi P., Padovani P., 2015, *MNRAS*, 450, 2404 (Paper IV)  
 Giovanoni P. M., Kazanas D., 1990, *Nature*, 345, 319  
 Glashow S. L., 1960, *Phys. Rev.*, 118, 316  
 Globus N., Allard D., Mochkovitch R., Parizot E., 2014, *MNRAS*, submitted (arXiv:1409.1271)  
 Glüsenskamp T., for the IceCube Collaboration, 2015, proceedings of the RICAP-14 conference, Noto, Sicily (arXiv:1502.03104)  
 Halzen F., Zas E., 1997, *ApJ*, 488, 669  
 High Resolution Fly'S Eye Collaboration, et al., 2009, *Astroparticle Physics*, 32, 53  
 IceCube Collaboration, 2013, *Science*, 342, 1242856  
 IceCube Collaboration, 2014, *Phys. Rev. Lett.*, 113, 101101  
 Kalashev O. E., Kusenko A., Essey W., 2013, *Phys. Rev. Lett.*, 111, 041103  
 Kelner S. R., Aharonian F. A., Bugayov V. V., 2006, *Phys. Rev. D*, 74, 034018  
 Kirk J. G., Mastichiadis A., 1989, *A&A*, 213, 75  
 Kistler M. D., Stanev T., Yüksel H., 2014, *Phys. Rev. D*, 90, 123006  
 Komatsu E., et al., 2011, *ApJS*, 192, 18

- Lacki B. C., Horiuchi S., Beacom J. F., 2014, *ApJ*, 786, 40
- Learned J. G., Pakvasa S., 1995, *Astroparticle Physics*, 3, 267
- Loeb A., Waxman E., 2006, *Journal of Cosmology and Astroparticle Physics*, 5, 003
- Mannheim K., Biermann P. L., Kruells W. M., 1991, *A&A*, 251, 723
- Mannheim K., Biermann P. L., 1992, *A&A*, 253, L21
- Mannheim K., 1993, *Phys. Rev. D*, 48, 2408
- Mannheim K., 1995, *Astroparticle Physics*, 3, 295
- Mannheim K., Protheroe R. J., Rachen J. P., 2001, *Phys. Rev. D*, 63, 023003
- Maraschi L., Ghisellini G., Celotti A., 1992, *ApJL*, 397, L5
- Mücke A., Rachen J. P., Engel R., Protheroe R. J., Stanev, T., 1999, *Publ. Astron. Soc. Austral.*, 16, 160
- Mücke A., Protheroe R. J., 2001, *Astroparticle Physics*, 15, 121
- Mücke A. et al., 2003, *Astroparticle Physics*, 18, 593
- Murase K., Inoue Y., Dermer C. D., 2014, *Phys. Rev. D*, 90, 023007
- Nolan P. L., et al., 2012, *ApJS*, 199, 31
- Padovani P., Giommi P., 1995, *ApJ*, 444, 567
- Padovani P., Resconi E., 2014, *MNRAS*, 443, 474
- Padovani P., Giommi P., 2015, *MNRAS*, 446, L41 (Paper III)
- Petropoulou M., Mastichiadis A., 2015, *MNRAS*, 447, 36
- Petropoulou M., Dimitrakoudis S., Padovani P., Mastichiadis A., Resconi E., 2015, *MNRAS*, 448, 2412
- Piran T., 2004, *Rev. of Mod. Phys.*, 76, 1143
- Planck Collaboration, 2011, *A&A*, 536, A16
- Plotkin R. M., Markoff S., Trager S. C., Anderson S. F., 2011, *MNRAS*, 413, 805
- Rachen J. P., Mészáros P., 1998, *Phys. Rev. D*, 58, 123005
- Reimer A., Böttcher M., Postnikov S., 2005, *ApJ*, 630, 186
- Sbarrato T., Ghisellini G., Maraschi L., Colpi M., 2012, *MNRAS*, 421, 1764
- Sbarrato T., Padovani P., Ghisellini G., 2014, *MNRAS*, 445, 81
- Sikora M., Begelman M. C., Rees M. J., 1994, *ApJ*, 421, 153
- Sironi L., Spitkovsky A., Arons J., 2013, *ApJ*, 771, 54
- Stecker F. W., 2007, *Journal of Physics: Conference Series*, 60, 215
- Tavecchio F., Ghisellini G., 2015, *MNRAS*, 451, 1502
- Urry C. M., Padovani P., 1995, *PASP*, 107, 803
- Zdziarski A. A., Böttcher M., 2015, *MNRAS*, 450, L21